

Report on Czech COSPAR-related activities in 2020-2021

This report summarizes selected results of five Czech institutions represented in the Czech National Committee of COSPAR, namely the Institute of Atmospheric Physics (IAP) of the Czech Academy of Sciences (CAS), the Astronomical Institute (AI) of CAS, the Faculty of Mathematics and Physics of the Charles University (FMP CU), the Faculty of Electrical Engineering of the Czech Technical University, and the SME company Iguassu (space industry, representing the Czech Space Alliance). Both selected scientific results and Czech participation in space experiments are reported. There are also significant outreach/PR activities.

Participation in space experiments

Astronomical Institute of the Czech Academy of Sciences (AI CAS):

Solar Orbiter. AI CAS was involved in building three scientific instruments for the Solar Orbiter ESA mission: hard X-ray telescope STIX, coronagraph METIS and plasma wave detector RPW. For STIX, the flight power supply and on-board software was delivered. The main optics composed from two mirrors was designed and manufactured in collaboration with TOPTEC (part of the Institute of Plasma Physics of CAS) for the METIS telescope. Finally, a low-voltage power supply and corresponding power distribution unit was developed and manufactured at AI CAS for the RPW detector. Solar Orbiter was successfully launched on 10th of February 2020 and all the instruments are working well. Currently we expect a first close approach to the Sun.

ATHENA. In 2019, the Czech team became a member of the international instrumentation consortium of the X-ray Integral Field Unit (X-IFU), the main instrument planned for the ESA large X-ray mission ATHENA (Advanced Telescope for High Energy Astronomy). The X-IFU instrument will use a novel technique of X-ray calorimetry to precisely measure energies of X-ray photons. The international consortium is led by France and has 13 countries participating in the consortium. The Czech team will be responsible for delivering a row-0 addressing module that will be part of warm electronics of the instrument. AI CAS is responsible for the project management and also for work in the X-IFU science advisory team. IAP CAS is responsible for the development of the electronics. In 2021, AI CAS got involved in development of the other detector onboard ATHENA mission, Wide Field Imager (WFI). The Czech team is responsible for the development of the Galvanic Isolation Modules. The ATHENA mission is currently in Phase B, waiting for the mission adoption expected in 2023.

LISA. The Czech Instrumental Group (CIG) joined the consortium of the large ESA gravitational-wave mission LISA (Laser Interferometer Space Antenna) in 2020. CIG is responsible for the development of the Fiber Switch Unit Actuators (FSUA). The FSUA will use piezo mechanisms to precisely rotate an optical element mounted in these mechanisms. By this rotation, the FSUA will be effectively able to switch between two sources of the laser beam, which guarantees the redundancy of the laser source. Since FSUA are critical elements for the LISA Optical Bench, CIG participates in the Interferometry Detection System of LISA mission. Apart from the mechanism itself, also the driving electronics and the box for the

Mission Control Unit will be subject of the delivery. CIG involves four institutes of CAS: AI, Institute of Physics, IAP and Institute of Thermomechanics.

eXTP. In 2019, the Czech team became a member of the international consortium of the Large Area Detector (LAD) planned for the Chinese-European enhanced X-ray Timing and Polarimetry mission eXTP. The eXTP mission will be devoted to measuring emission from matter in extremely strong gravitational and magnetic fields. The LAD instrument will use a very large collecting area to obtain high signal-to-noise to set tight constraints on the measured parameters. The LAD consortium is led by Italy and the Czech team will be responsible for design and manufacturing of the detector and collimator frames. AI CAS is leading the project in collaboration with the industrial company Elya and the Silesian University in Opava. The main industrial partner composed of two Czech companies, Frentech and L.K.Engineering, was selected by ESA in a tender. The project is currently in Phase B. A potential involvement of ESA is the subject of ongoing negotiations. The instrument LAD was recently redesigned. The required changes are reflected in a project update and will be subject to approval by the Czech ministries. There has been significant progress on the theory and modelling side of strong-gravity signatures in X-ray polarisation. The results of the current phase were delivered during the 43rd COSPAR Scientific Assembly in 2021 and reviewed in *Advances in Space Research* 69, 448-466 (2022).

IXPE. The Czech scientific team is also involved in the exploratory NASA mission IXPE (Imaging X-ray Polarimetry Explorer) that was launched on 9th of December 2021. The Czech team contributed to the definition of the science program during the commissioning phase and is participating in the first data analysis.

Juice. On JUICE mission the Czech team is a member of the international consortium for the Radio and Plasma Waves Instrument (RPWI). The responsibility of the ASU team was to perform the full development of a custom made low voltage power supply under very strict EMC requirements in order to provide reliable and unperturbed scientific measurements. In 2020 the flight HW was successfully delivered to the RPWI PI institute (IRFU, Sweden), later on followed with delivery of the spare HW units in 2021. The complete RPWI is now integrated on the JUICE spacecraft and passed so far all pre-flight on ground tests campaigns. The launch of the mission is currently scheduled in mid of 2022.

PLATO. The Czech Republic became a member of the PLATO mission consortium in 2019. The Czech Republic has a representative in the PLATO mission board and the Astronomical Institute contributes by software which helps to correct the systematic effects. Furthermore, a company SAB Aerospace was subcontracted to deliver the transport containers for PLATO cameras. In terms of science, AI CAS is currently installing a new spectrograph PLATOSpec at La Silla observatory on E152 telescope. PLATOSpec will serve as a ground-based support of the PLATO space mission and it will help with the follow-up of planetary candidates from PLATO mission. Involvement in the PLATO mission consortium will help increasing the significance of the growing Czech exoplanetary community.

PROBA-3. Czech team continued in the manufacturing of the flight models of the Front Door Assembly and the optical components of the coronagraph ASPIICS onboard PROBA-3. In 2021, flight models were delivered to the instrument prime contractor CSL (Belgium). The launch is expected in 2023.

Earth observation. The Planetary Systems group of ASU has been participating both in international and Czech projects related to Earth observation. We contribute to the international consortium of five science institutes led by TU Delft that supplies gravity field solutions to ESA. Such fields are based on high precision GPS orbits of Swarm satellites (ESA mission) and the Czech side contributes with an independent method (de-correlated acceleration approach). Besides processing of magnetometry data from Swarm, data and products from the missions GRACE and GRACE-FO (US-GER missions), dedicated to the global mass transport typically associated with large water mass variations (seasonal cycle, ice melting, groundwater, etc.), are processed. Such data gives the only picture of the total changes of mass distribution within the Earth (with the largest changes near the surface). Satellite gravimetry data are also used with terrestrial high-resolution gravimetry maps for geophysical prospection (hidden lakes, volcanoes etc.). Besides satellite data processing, the group has been working on the analyses of Earth rotation (data from IERS) to inspect the role of geomagnetic jerks, and, on Earth orientation with help from the VLBI data (Very Long Baseline Interferometry). The Earth rotation and the Earth orientation are used for setting up the global reference frames and the relation between terrestrial and celestial reference frames.

ESA Voyage 2050. We contributed to new mission proposals for the ESA Voyage 2050 program. One of the successful proposals selected for further investigation was proposal of an X-ray Interferometer (Uttley et al., 2020, SPIE, 11444, 17, <https://ui.adsabs.harvard.edu/abs/2020SPIE11444E..1EU/abstract>), a constellation of X-ray satellites that would resolve 1 microarcsec in X-rays and thus exceed the resolution of the Event Horizon Telescope and at the same time reaching the high-energy emission that is released by very energetic processes at the closest neighborhood of a black hole.

Institute of Atmospheric Physics of the Czech Academy of Sciences (IAP CAS):

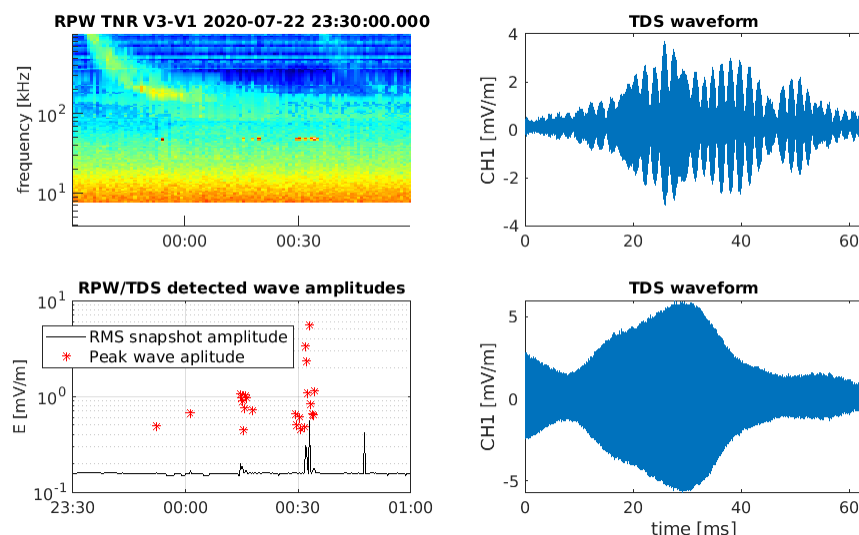


Fig. 1. Solar Orbiter RPW observations of a Type III radio burst, showing Langmuir waves detected by the TDS module.

In February 2020, the European Space Agency (ESA) launched a Solar Orbiter mission to the inner heliosphere. The spacecraft carries a Radio and Plasma Waves instrument (RPW) which includes a Time Domain Sampler (TDS) subsystem developed at the Institute of Atmospheric

Physics in Prague. The instrument, including the TDS module, has been operating successfully since the beginning of the mission and already provided data from several perihelium passes as well as two Venus flybys.

The scientific and engineering team at IAP is preparing an important hardware contribution to the future Comet Interceptor mission of ESA, which aims to investigate a dynamically new comet during its first approach to the Sun. IAP is developing a Dust and Data Processing Unit, an on-board computer implementing processing and compression of data from multiple sensors of the Dust, Field and Plasma instrument as well as FPGA-based signal processing to detect signatures of cometary dust impacts in electric field data.

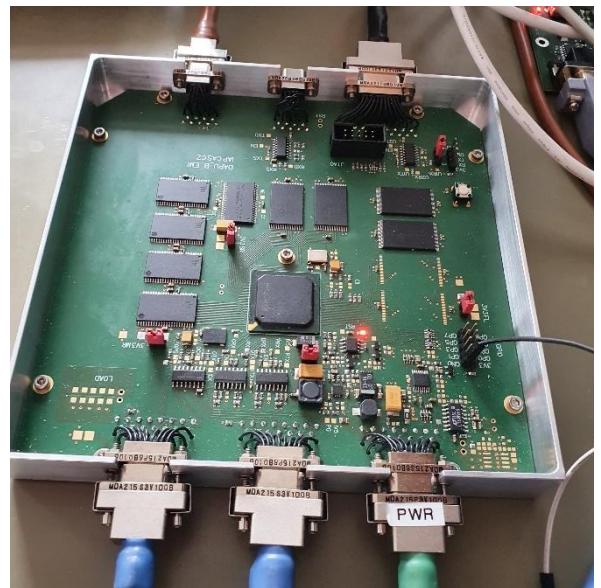


Fig. 2. A prototype of the DAPU data processing unit for the Dust, Field and Plasma instrument for the Comet Interceptor spacecraft.

The Department of Space Physics of the Institute of Atmospheric Physics of the Czech Academy of sciences is also involved as a Co-PI team in the RPWI (Radio and Plasma Waves Investigation) instrument of JUICE (JUperiter ICy moons Explorer) mission. The mission is scheduled for launch in 2023, aiming at investigation of the Jovian system and its three Galilean icy moons (Europa, Ganymed and Callisto). The RPWI instrument is developed in a consortium lead by the Swedish Institute of Space Physics, Uppsala, Sweden. The IAP team focuses on research of electromagnetic waves in the Jovian magnetosphere and in the vicinity of Jovian moons using the LFR (Low Frequency Receiver) which will provide us with multi-component measurements of electromagnetic fields at frequencies up to 20 kHz.

IAP is also involved in development of space electronics also for the large astrophysics missions of ESA, Athena and LISA, in collaboration with other institutes of the Czech Academy of Sciences.



Fig. 3. The ESA JUICE mission.

Reception of the telemetry data of the WBD instrument onboard four ESA Cluster spacecraft continues in the Panska Ves station of the IAP. The data were processed at IAP CAS and submitted to international scientific community.

In 2020 two international space missions were launched, where FMP CU had participated in the scientific payload development. In February 2020, the ESA mission Solar Orbiter started its several year journey to the Sun. Charles University had been involved in development of the SWA/PAS proton and alpha particle sensor that currently delivers unique 3D ion velocity spectra with 4 s time resolution (normal mode) and provides 250 ms resolved 3D spectra during burst mode.

The French satellite TARANIS with the energetic electron spectrometer IDEE, developed also with the participation of Charles University (data processing unit), was dedicated to investigations of transient luminous phenomena above thunderstorm clouds. Unfortunately, its launch in November 2020 was unsuccessful because of the Vega launcher failure.

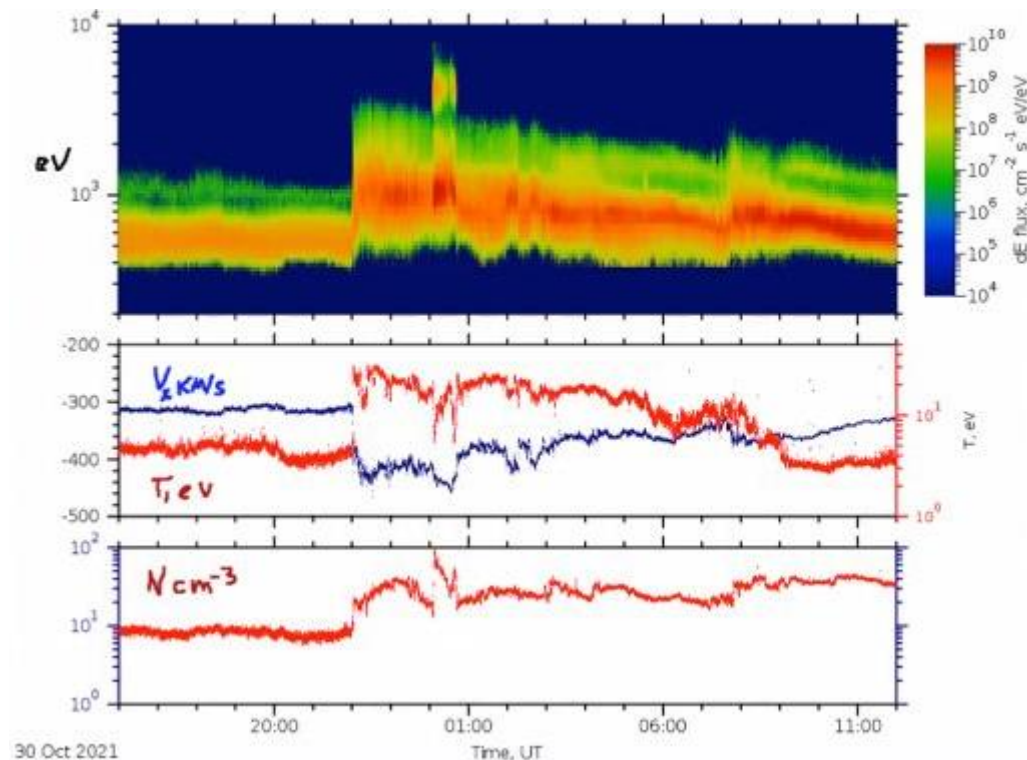


Fig. 4. Solar Orbiter SWA/PAS observation of the interplanetary shock on Oct. 31, 2021.

Since 2019 we have been involved in the ESA Fast mission Comet Interceptor aiming to flyby near a dynamically new object (a comet or an extra-solar origin body). The mission was passing the A/B development phases during 2020-2021. In this mission we will provide part of the electronics of the electron spectrometer LEES (the 3D low-energy electron spectrometer led by IRAP Toulouse). The launch is currently planned in 2029.

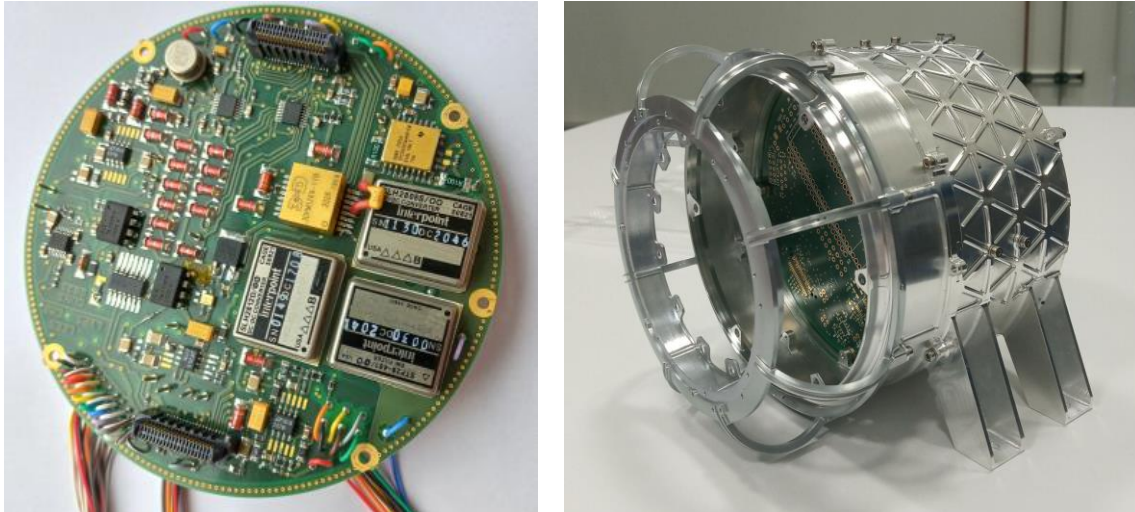


Fig. 5. The LEES low-voltage power supply EM0 board developed at Charles University and the LEES prototype mechanics during AIT in IRAP Toulouse.

During 2020-2021 Charles University also worked on development of several Faraday-cup based solar wind monitor instruments (BMSW-LG/BMSW-S for the Russian Luna-Resurs-1 OA and Strannik missions) and a smaller version for the Italian HENON cubesat mission.

Iguassu Software Systems, a.s.

Galileo, EGNOS V2 and V3 projects for EUSPA – ongoing. Member of two consortia. One project is with Thales Alenia Space, in continued development of our EGNOS/SBAS performance monitoring software EVORA. The quality and innovativeness of the software is underlined by the fact that TAS gave us a 4 year contract for continuing enhancements development. This contract is now being extended for further 4 years. Apart from TAS, the software is being used by other major European GNSS primes, ESA as well as the Japanese government institute responsible for the QZSS constellation. The other GNSS project is development with SpaceOpal of HAUT – high accuracy user terminal for Galileo High Accuracy Service. Next activity for EGNOS V2 and V3 is the development of EGNOS performance tool under the subcontract with ESSP. Iguassu is also developing a SW to predict EGNOS performance using the Machine Learning.

Space Situational Awareness Safety for ESA. Several projects completed, e.g. qualification of optical sensors with Matera and the Teplice observatory. Other three ongoing to develop better technology to monitor NEOs - Near Earth Objects. We are priming some of the projects, with an international team including Spain, Poland and Romania. The TBT – test bed telescope – consists of two observatories, one of which is operating in Spain and the other being commissioned in ESO, Chile. The telescopes and the dome operate fully autonomously to detect, track, and refine orbits of NEOs. Our contribution is the software which analyses the images, detects objects, calculates their trajectory and refines the latter with automatic follow-up observations. Another detection device is the fly-eye telescope being developed under ESA contract, where we develop similar functionality. Iguassu is continuing the work on TBT in two parallel CCNs, where in the first one processing SW updates were performed and in the second one Iguassu S2P expertise is used to help Slovak entities in the PECS program. Another activity was to define and implement scheduling standards for space debris observation under the POSST project.

Iguassu is also member of European Optical Network (EON), reviewing standards and developing SW for space debris processing. Another activity is CREAM 3 where Iguassu is contributing to the backend development of collision avoidance risk database.

ARIANE 6 – ongoing. Iguassu is a member of two consortiums developing the launcher and the ground segment telemetry processing. The launcher telemetry processing is specific in that it requires innovative selection of key critical data, to cope with the decreasing transmitted bandwidth as the distance of the launcher from the launch pad rapidly increases.

BBT - Materials Processing, Ltd.

IAPETHOS 2 (BBT) – to be finished in 2022. The main strategic objective of IAPETHOS 2 was to design, develop, and subsequently initiate the commercial production of the new types of advanced optical Calomel-based polarizers (Wollaston, Rochon, Senarmont, optical depolarizer/scrambler and lossless polarizer as a unique BBT original design) for the MWIR and LWIR spectral regions. Furthermore, in collaboration with external partners, an effective anti-reflective coating and bonding solution (optical immersion) has been developed to find a true protective AR layer with long-lasting adhesion.

BITRAS (BBT) - to be finished in 2022. BITRAS project was focused on R&D with a view to producing prototypes of Calomel prisms that will find applications in the global optical and photonic markets as materials for use in the mid- and far-infrared region, especially in the design of hybrid interferometers and spectroscopic instruments.

ECLIPSE (BBT) - completed in 2021. The project was aimed at improving the production capacity and quality of IR Calomel-based polarizers. The main technical objective was to increase the technology readiness level (TRL) of recently developed polarizers (breadboards), to demonstrate critical functions of the element in a relevant environment. As a requirement the developed polarizers had to demonstrate an Extinction Ratio ER higher than 1:20000 for MWIR and 1:10000 for LWIR spectral regions.

POFILASE (FUTONICS, BBT, KOSET, LZH, COPTI) - completed in 2021. The aim of the POFILASE project was to develop a fibre continuous wave laser with a wavelength of 2 μm and a power of 350 W for industrial applications such as welding of plastics and machining of composite and other materials. Our participation in the project/consortium involved the development and integration of an optical isolator capable of handling light output.

TWINS (CNR, BBT, NIREOS) – started in 2022. We have recently started work on the development of a lightweight and ultra-compact FT spectrometer. Current cosmic TIR imagers use bandpass filters and only acquire maps at a discrete number of predefined wavelengths, limiting chemical identification capabilities. Therefore, we propose a hyperspectral imager that is capable of capturing continuous TIR spectra, which greatly expands the range of applications.

Selected scientific results

Multipoint measurements of whistler-mode waves in the Earth's magnetosphere: hiss originating in whistlers. Measurements of electromagnetic waves in space plasmas are an important tool for our understanding of physical processes in this environment. We used multi-point measurements of electromagnetic field fluctuations by the Cluster space fleet to discuss sources of plasmaspheric hiss. Our case study shows hiss which was triggered in the dayside outer plasmasphere by non-ducted whistlers emitted from strong lightning strokes. Spectral properties of magnetospherically reflecting whistlers and hiss strongly depend on geographical location of the source. We also showed results collected during a close conjunction of the Van Allen Probes and Arase spacecraft. The inter-calibration was based on a fortuitous case of common observations of strong whistlers at frequencies between a few hundred hertz and 10 kHz, which were generated by the same lightning strokes and which propagated along very similar paths to the two spacecraft.

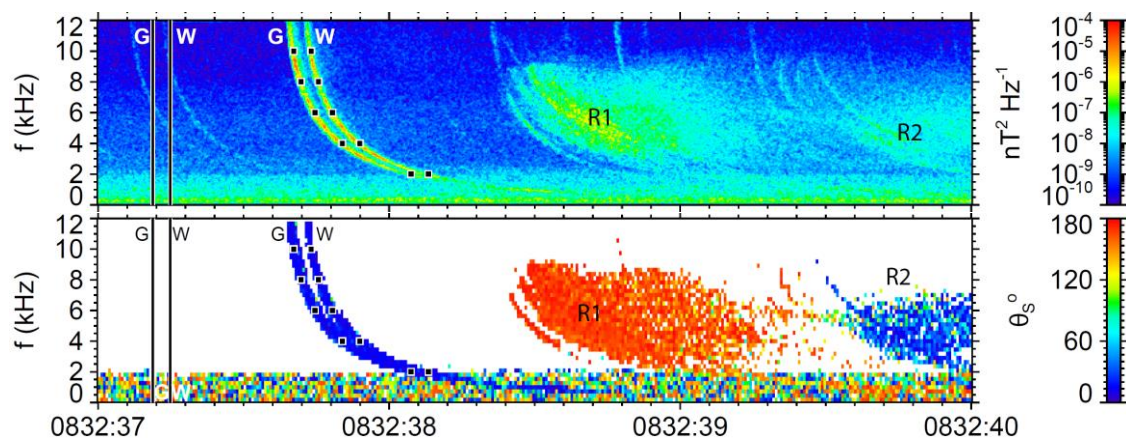


Fig. 6. Observations of strong whistlers by the Van Allen Probe B spacecraft. Top: total power spectral density of magnetic field fluctuations obtained as the trace of the magnetic spectral matrix; bottom: angle between the spectral estimate of the Poynting vector and the vector of the background magnetic field.

Santolík, O., Kolmašová, I., Pickett, J. S., & Gurnett, D. A. (2021). Multi-point observation of hiss emerging from lightning whistlers. *Journal of Geophysical Research: Space Physics*, 126, e2021JA029524. <https://doi.org/10.1029/2021JA029524>.

Santolík, O., Miyoshi, Y., Kolmašová, I., Matsuda, S., Hospodarsky, G. B., Hartley, D. P., et al. (2021). Inter-calibrated measurements of intense whistlers by Arase and Van Allen Probes. *Journal of Geophysical Research: Space Physics*, 126, e2021JA029700. <https://doi.org/10.1029/2021JA029700>.

The Faraday rotation effect in Saturn Kilometric Radiation observed by the Cassini spacecraft.

Non-thermal radio emissions from Saturn, known as Saturn Kilometric Radiation (SKR), were analyzed for the Faraday rotation effect detected in Cassini RPWS High Frequency Receiver (HFR) observations. This phenomenon, which mainly affects the lower-frequency part of SKR below 200 kHz, is characterized by a rotation of the semi-major axis of the SKR polarization ellipse as a function of frequency during wave propagation through a birefringent plasma medium. Faraday rotation was found in 4.1% of all HFR data recorded by Cassini above 20 degrees northern and southern magnetic latitude, from mid-2004 to late 2017. A statistical visibility analysis has shown that elliptically polarized SKR

from the dawn source regions, when beamed toward high latitudes into the noon and afternoon local time sectors, is most likely to experience Faraday rotation along the ray path. The necessary conditions for Faraday rotation were discussed in terms of birefringent media and sharp plasma density gradients, where SKR (mostly R-X mode) gets split into the two circularly polarized modes R-X and L-O. By means of a case study we also demonstrated how Faraday rotation provides an estimate for the average plasma density along the ray path.

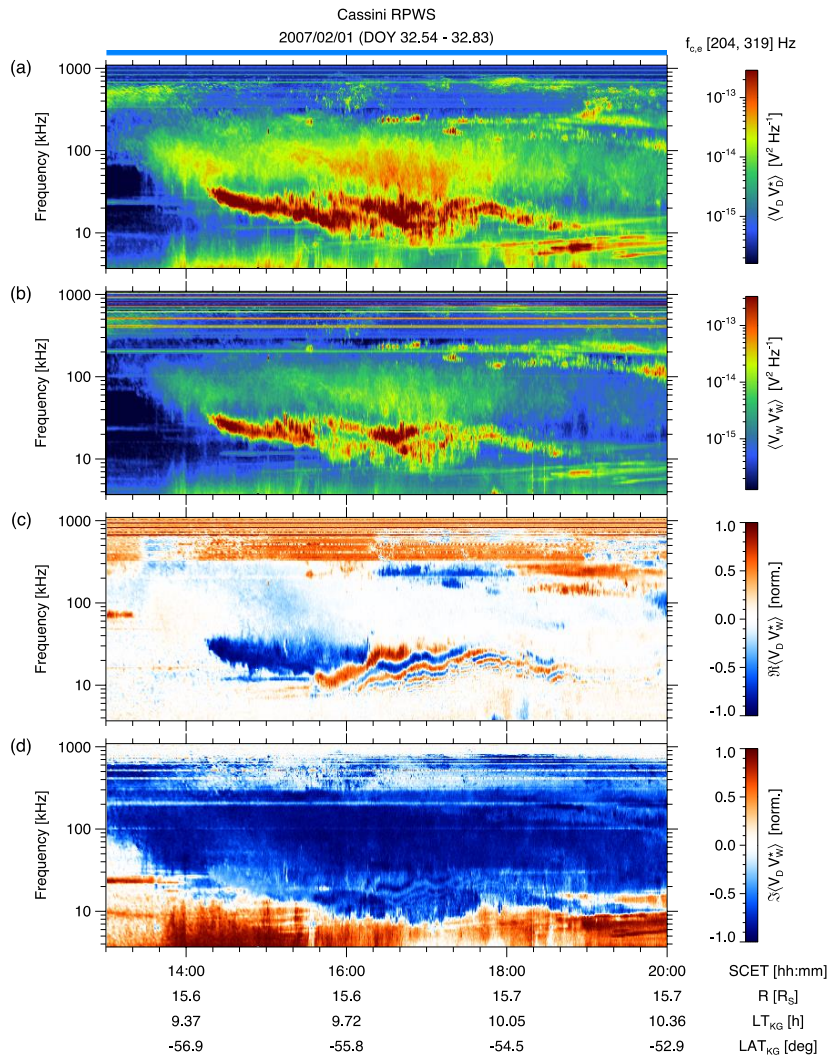


Fig. 7. A summary of Cassini RPWS/HFR observations in 2-antenna mode from February 1, 2007. (a) Auto-power spectral density in the dipole antenna, (b) auto-power spectral density in the w-antenna, (c) real part (including Faraday fringes) and (d) imaginary part of the cross-power spectral density between both antennas. Time and spacecraft coordinates (kronographic) are given at the bottom. Modulations of SKR emission by Faraday rotation are clearly visible in (c) between 7 and 30 kHz as oscillations of $Re\langle V_D V_w^* \rangle$ between -1 (blue) and +1 (red).

Taubenschuss, U., Lamy, L., Fischer, G., Piša, D., Santolík, O., Souček, J., Kurth, W. S., Cecconi, B., Zarka, P., Rucker, H. O. (2021). The Faraday rotation effect in Saturn Kilometric Radiation observed by the CASSINI spacecraft. *Icarus*, 370, 114661. <https://doi.org/10.1016/j.icarus.2021.114661>

Measurability of the nonlinear response of electron distribution function to chorus emissions in the Earth's radiation belt. The whistler-mode chorus waves are known to have a major impact on the dynamics of the Earth's outer radiation belt, causing acceleration

and loss of energetic electrons. In this paper we focused on the possibility of analyzing the nonlinear properties of chorus through measurements of perturbations in the hot electron velocity distribution caused by interaction with the waves. We used a recently developed model of a single rising-tone chorus element with a sub-packet structure and employed backward-in-time test particle simulations to obtain the perturbed electron distribution. We then analyzed the character and magnitude of these perturbations and assessed their measurability.

It was found that the nonlinear interaction of chorus sub-packets with electrons causes the creation of stripes of increased and decreased phase space density. These stripes are initially aligned to resonance velocity curves, but become distorted due to the adiabatic motion of the electrons, and their structure further becomes less clear as the frequency of the chorus riser increases. On the front of the perturbation region, a prominent decrease in phase space density, associated with the electromagnetic electron hole, can be observed. We calculated the particle fluxes in our simulation and estimated the particle counts which could be measured by the state-of-art electrostatic analyzers on spacecraft. We concluded that no recent particle instrument has the necessary pitch angle resolution and geometric factor to make a significant observation. A new instrument with improved angular resolution is needed to measure the perturbations predicted by our simulations. A successful observation would confirm the validity of previous theoretical predictions, and it could also partially reconcile two major theories of chorus growth, the nonlinear growth theory and the backward-wave oscillator theory.

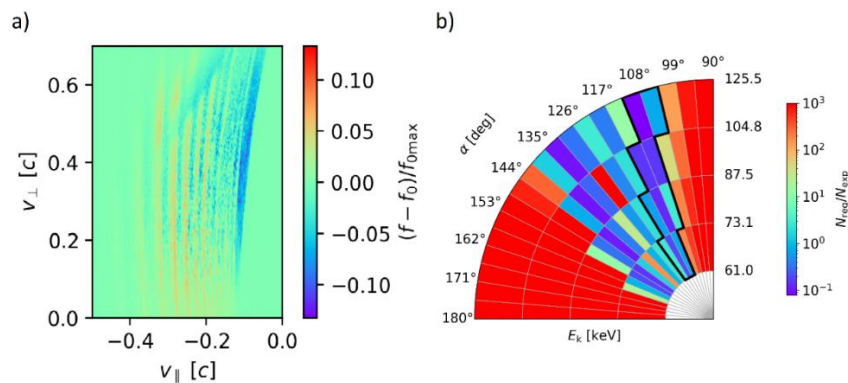
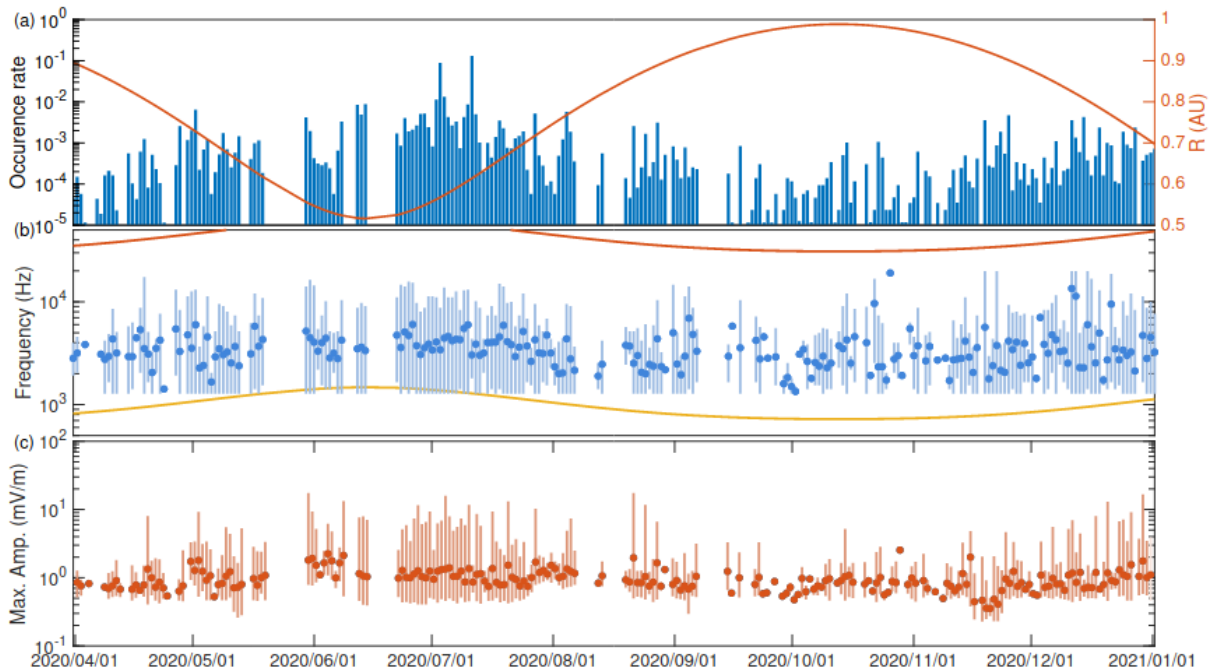


Fig. 8. (a) Perturbations of hot electron velocity distribution after interaction with a chorus element, as captured at the magnetic equator right after the last subpacket. The plot shows a normalized difference between the perturbed distribution and the initial distribution. (b) Polar plot in energy-pitch angle space showing the ratio N_{req}/N_{exp} , where N_{req} is the number of particles required to make a 1-sigma significant measurement of the perturbations, and N_{exp} is the number of particles expected to be measured by an electrostatic particle analyzer.

Hanzelka, M., O. Santolík, Y. Omura, I. Kolmašová (2021), Measurability of the nonlinear response of electron distribution function to chorus emissions in the Earth's radiation belt, *J. Geophys. Res. Space Physics*, e2021JA029624, doi: 10.1029/2021JA029419.

Plasma waves and interplanetary dust in the solar wind: new measurements of the Time Domain Sampler module within the Radio and Plasma Waves instrument onboard Solar Orbiter. The Radio and Plasma Waves instrument, including the Time Domain Sampler, has been measuring electromagnetic phenomena in the solar wind nearly continuously since the start of Solar Orbiter in February 2020. Data from the Czech instrument, obtained at a range of heliocentric distances, resulted in several studies of high frequency waves in the solar wind



plasma and a study of interplanetary dust, deriving for the first time the average radial velocity of dust grains.

Fig. 9. Wave emission observed by the Time Domain Sampler of the Radio and Plasma Waves instrument onboard Solar Orbiter: (a) blue bars show the occurrence rate of intense waves below 20 kHz, over-plotted orange line representing the distance from the Sun; (b) distribution of observed wave frequencies with their observed minimum-maximum range, orange and yellow lines respectively represent modelled electron and proton plasma frequencies; (c) averaged maxima of wave amplitudes with their range.

J. Souček, D. Piša, I. Kolmašová, L. Uhlíř, R. Lán, O. Santolík, V. Krupař, O. Krupařová, J. Baše, M. Maksimovic, S. D. Bale, T. Chust, Yu. V. Khotyaintsev, V. Krasnoselskikh, M. Kretzschmar, E. Lorfèvre, D. Plettemeier, M. Steller, Š. Štverák, A. Vaivads, A. Vecchio, D. Bérard and X. Bonnin, Solar Orbiter Radio and Plasma Waves – Time Domain Sampler: In-flight performance and first results, *A&A*, 656 (2021) A26, <https://doi.org/10.1051/0004-6361/202140948>.

D. Piša, J. Souček, O. Santolík, M. Hanzelka, G. Nicolaou, M. Maksimovic, S. D. Bale, T. Chust, Y. Khotyaintsev, V. Krasnoselskikh, M. Kretzschmar, E. Lorfèvre, D. Plettemeier, M. Steller, Š. Štverák, P. Trávníček, A. Vaivads, A. Vecchio, T. Horbury, H. O'Brien, V. Evans, V. Angelini, C. J. Owen and P. Louarn, First-year ion-acoustic wave observations in the solar wind by the RPW/TDS instrument on board Solar Orbiter, *A&A*, 656 (2021) A14, <https://doi.org/10.1051/0004-6361/202140928>.

A. Zaslavsky, I. Mann, J. Souček, A. Czechowski, D. Piša, J. Vaverka, N. Meyer-Vernet, M. Maksimovic, E. Lorfèvre, K. Issautier, K. Rackovic Babic, S. D. Bale, M. Morooka, A. Vecchio, T. Chust, Y. Khotyaintsev, V. Krasnoselskikh, M. Kretzschmar, D. Plettemeier, M. Steller, Š. Štverák, P. Trávníček and A. Vaivads, First dust measurements with the

Occurrence of electromagnetic ion cyclotron waves in the magnetosphere according to their distance to the magnetopause. Wave growth of electromagnetic ion cyclotron (EMIC) emissions observed in the outer magnetosphere is mainly controlled by compression events resulting from solar wind dynamic pressure pulses. During such events wave growth is expected to be maximum close to the magnetopause. In previous studies, distribution of EMIC waves was analyzed according to their distance from the Earth, which is inadequate for studying the magnetopause region. We mapped a data set of EMIC waves observed by the THEMIS spacecraft according to their distance from a case-by-case modeled magnetopause. EMIC occurrence rate was found to be maximum within two Earth radii from the magnetopause and then it linearly decreased with the increasing distance, especially close to the local noon.

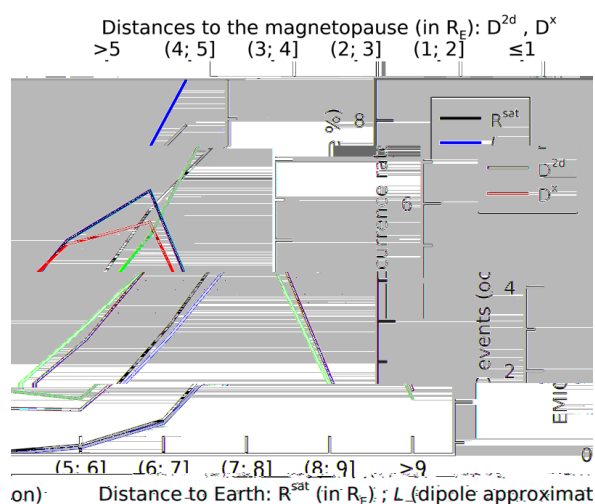


Fig. 10. Occurrence rate (right panel) of EMIC events observed up to 10 Earth radii (RE) between 8 and 16 MLT, by the THEMIS spacecraft. Results are presented as a function of L (in red), the distance to Earth R^{sat} (in black) or to the modelled magnetopause (absolute distance D^{2d} in green and distance toward the Sun D^x in blue). Upper and lower abscissa have opposite orientations to make comparisons easier.

Grison, B., Santolík, O., Lukačević, J., & Usanova, M. E. (2021). Occurrence of EMIC waves in the magnetosphere according to their distance to the magnetopause. *Geophysical Research Letters*, 48, e2020GL090921. <https://doi.org/10.1029/2020GL090921>

Radio and plasma waves in the vicinity of Venus and whistler-mode waves in the solar wind.

On December 27, 2020, Solar Orbiter completed its first gravity assist maneuver of Venus. While this flyby was performed to provide the spacecraft with sufficient velocity to get closer to the Sun and observe its poles from progressively higher inclinations, the Radio and Plasma Wave (RPW) consortium, along with other operational in-situ instruments, had the opportunity to perform high cadence measurements and study the plasma properties in the induced magnetosphere of Venus (Hadid et al 2021). These observations include the identification of a number of magnetospheric plasma wave modes, measurements of the electron number densities computed using the quasi-thermal noise spectroscopy technique and inferred from the probe-to-spacecraft potential, the observation of dust impact signatures,

kinetic solitary structures, and localized structures at the bow-shock, in addition to the validation of the wave normal analysis on-board from the Low Frequency Receiver. Our contribution to the development of algorithms for this module was also reflected by new results on the whistler mode waves in the solar wind (Chust et al, 2021; Kretzschmar et al, 2021).

- L. Z. Hadid, N. J. T. Edberg, T. Chust, D. Píša, A. P. Dimmock, M. W. Morooka, M. Maksimovic, Yu. V. Khotyaintsev, J. Souček, M. Kretzschmar, A. Vecchio, O. Le Contel, A. Retino, R. C. Allen, M. Volwerk, C. M. Fowler, L. Sorriso-Valvo, T. Karlsson, O. Santolík, I. Kolmašová, F. Sahraoui, K. Stergiopoulou, X. Moussas, K. Issautier, R. M. Dewey, M. Klein Wolt, O. E. Malandraki, E. P. Kontar, G. G. Howes, S. D. Bale, T. S. Horbury, M. Martinović, A. Vaivads, V. Krasnoselskikh, E. Lorfèvre, D. Plettemeier, M. Steller, Š. Štverák, P. Trávníček, H. O'Brien, V. Evans, V. Angelini, M. C. Velli and I. Zouganelis, Solar Orbiter's first Venus flyby: Observations from the Radio and Plasma Wave instrument, *A&A*, 656 (2021) A18, <https://doi.org/10.1051/0004-6361/202140934>
- T. Chust, M. Kretzschmar, D. B. Graham, O. Le Contel, A. Retinò, A. Alexandrova, M. Berthomier, L. Z. Hadid, F. Sahraoui, A. Jeandet, P. Leroy, J.-C. Pellion, V. Bouzid, B. Katra, R. Piberne, Yu. V. Khotyaintsev, A. Vaivads, V. Krasnoselskikh, **J. Souček**, **O. Santolík**, E. Lorfèvre, D. Plettemeier, M. Steller, Š. Štverák, P. Trávníček, A. Vecchio, M. Maksimovic, S. D. Bale, T. S. Horbury, H. O'Brien, V. Evans and V. Angelini, Observations of whistler mode waves by Solar Orbiter's RPW Low Frequency Receiver (LFR): In-flight performance and first results, *A&A*, 656 (2021) A17 DOI: <https://doi.org/10.1051/0004-6361/202140932>
- M. Kretzschmar, T. Chust, V. Krasnoselskikh, D. Graham, L. Colombari, M. Maksimovic, Yu. V. Khotyaintsev, **J. Souček**, K. Steinvall, **O. Santolík**, G. Jannet, J.-Y. Brochet, O. Le Contel, A. Vecchio, X. Bonnin, S. D. Bale, C. Froment, A. Larosa, M. Bergerard-Timofeeva, P. Ferreau, E. Lorfèvre, D. Plettemeier, M. Steller, Š. Štverák, P. Trávníček, A. Vaivads, T. S. Horbury, H. O'Brien, V. Evans, V. Angelini, C. J. Owen and P. Louarn, Whistler waves observed by Solar Orbiter/RPW between 0.5 AU and 1 AU, *A&A*, 656 (2021) A24, DOI: <https://doi.org/10.1051/0004-6361/202140945>

A new global empirical model of ion temperature for the International Reference Ionosphere. We developed a new global model of ion temperature (T_i), which represents a substantial improvement of current T_i representation in the International Reference Ionosphere (IRI-2016 the latest version). The model is based on a data base comprising almost all available satellite T_i data obtained by means of RPA (Retarding Potential Analyzer) measurement, i.e. data from 18 satellites. The used satellite data were corrected using comparisons with T_i data from long term measurements made by three incoherent scatter radars (ISRs) (Jicamarca, Arecibo, and Millstone Hill). The altitude range described by the model ranges from 350 km to 850 km covering the region where generally T_i is higher than the neutral temperature (T_n) and lower than the electron temperature (T_e). For altitudes above 850 km and below 350 km an extrapolation is used in such a way that at high altitudes T_i merges to T_e and at low altitudes T_i merges to T_n (T_e is calculated from TBT-2012 and T_n from NRLMSIS-00 (i.e., CIRA); both these models are part of the IRI code). The new model fully includes variation of T_i with the solar activity, better describes variation of T_i with local time (magnetic local time) and also describes T_i morning enhancement at the geomagnetic equator.

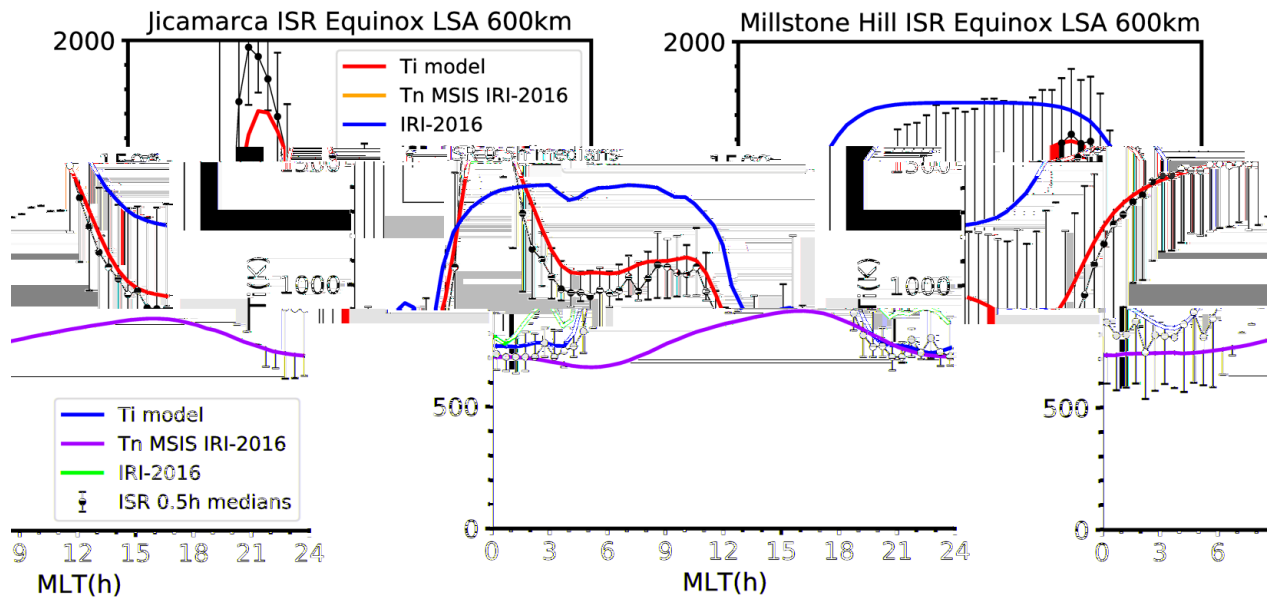
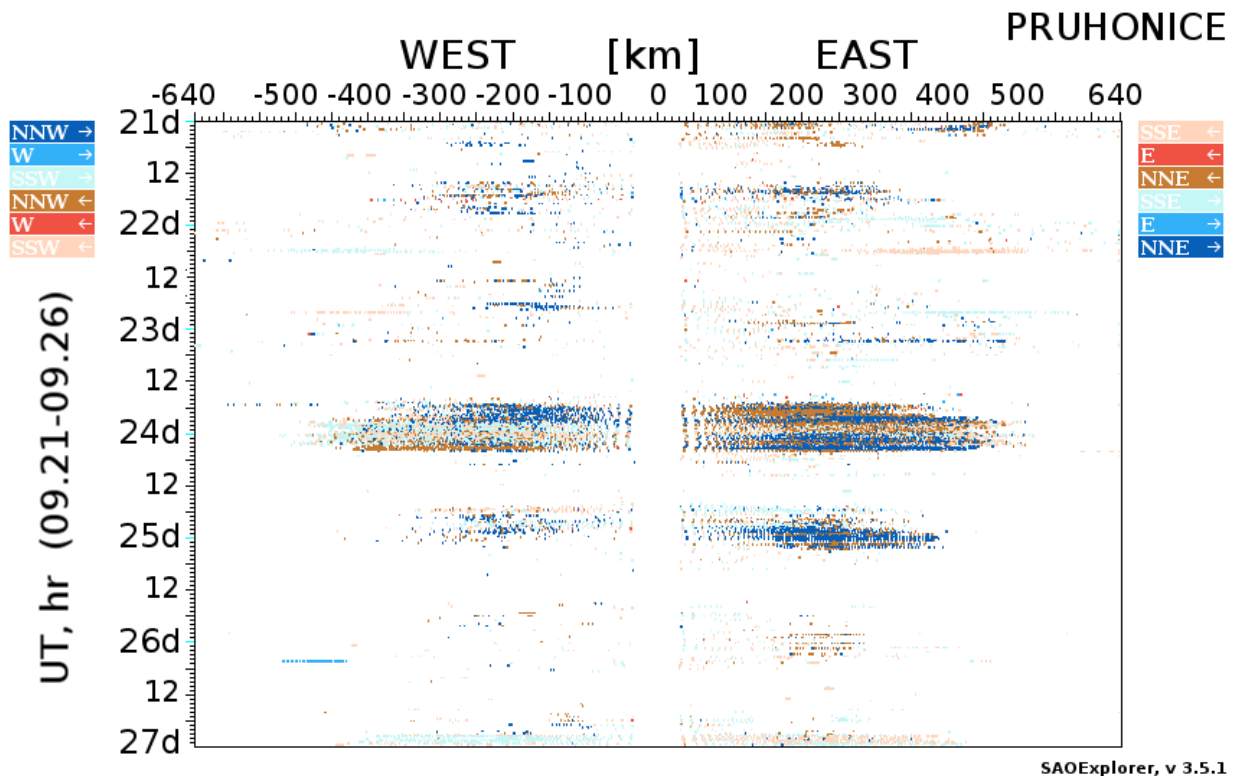


Fig. 11. An example of comparison of T_i dependence on local time (MLT) at an altitude of 600 km for equinox and low solar activity ($PF_{10.7} = 82.5$) according to the new model (solid red line), IRI-2016 (solid blue line) and from two ISRs (Jicamarca - left panel, Millstone Hill - right panel; black circles—medians, error bars—upper/lower quartile). T_n from NRLMSIS-00 is shown as well (solid orange line). At the geomagnetic equator (left panel) it is apparent that the new model describes well the T_i morning enhancement (maximum between 6 and 7 h MLT), while this feature is not included in IRI-2016.

Truhlík, V.; Bilitza, D.; Kotov, D.; Shulha, M.; Třísková, L. A Global Empirical Model of the Ion Temperature in the Ionosphere for the International Reference Ionosphere. *Atmosphere* **2021**, *12*, 1081. <https://doi.org/10.3390/atmos12081081>.

Evidence of vertical coupling: meteorological storm Fabienne and its related effects observed up to the ionosphere. Meteorological systems are assumed to be important source of wavy oscillations in the atmosphere. They can propagate from its source up to ionospheric heights. A pronounced frontal system associated with high thunderstorm activity crossed Europe on 23-24 September 2018. It moved with speed of $100\text{--}110 \text{ km h}^{-1}$. Related considerable changes were observed in stratospheric circulation over Europe. The zonal wind at 1 and 0.1 hPa levels changed from a typical westward circulation before storm to eastward after storm. We observed increased wave activity in the ionosphere shortly after crossing the frontal storm region border in dates of digisonde. Shortly after crossing a principal increase of the horizontal component of plasma motion (Fig. XA) and to pronounced decrease of vertical velocity of plasma motion appeared. Ionospheric observations were partly affected by recovery of a weaker geomagnetic storm. With respect to the principal change in stratospheric circulation we consider the observed wavy effects in the ionosphere to be excited by crossing of the cyclonic system Fabienne.



SAOExplorer, v 3.5.1

Fig. 12. Directogram showing the plasma motion in the ionosphere. Substantial enhancement immediately after the storm system is well visible.

P. Koucká Knížová, K. Podolská, K. Potužníková, D. Kouba, Z. Mošna, J. Boška, and M. Kozubek (2020): Evidence of vertical coupling: meteorological storm Fabienne on 23 September 2018 and its related effects observed up to the ionosphere. *Ann. Geophys.*, 38, 73–93, <https://doi.org/10.5194/angeo-38-73-2020>.

The best solar activity proxy for long-term ionospheric investigations. To select the best solar activity proxy is important for long-term trend or climatological studies of ionospheric parameters as well as for modeling. Solar proxies for foF2 and foE analyses are examined. The yearly average and monthly median values of foF2 and yearly values of foE of four European stations with long and high-quality data series are used. Six solar proxies are utilized: F10.7, F30, Mg II, He II, sunspot numbers and Lyman-. Mg II and F30 are found to be the best solar proxies for both yearly and monthly foF2 values. On the other hand, F10.7 is found to be the best solar proxy for yearly values of foE. The variability of yearly values of foF2 and foE is almost fully described (99%) by the best solar proxies and this relation is highly linear. Different solar proxies applied might result in somewhat different long-term trends of both foF2 and foE and they should affect also climatological and modelling results

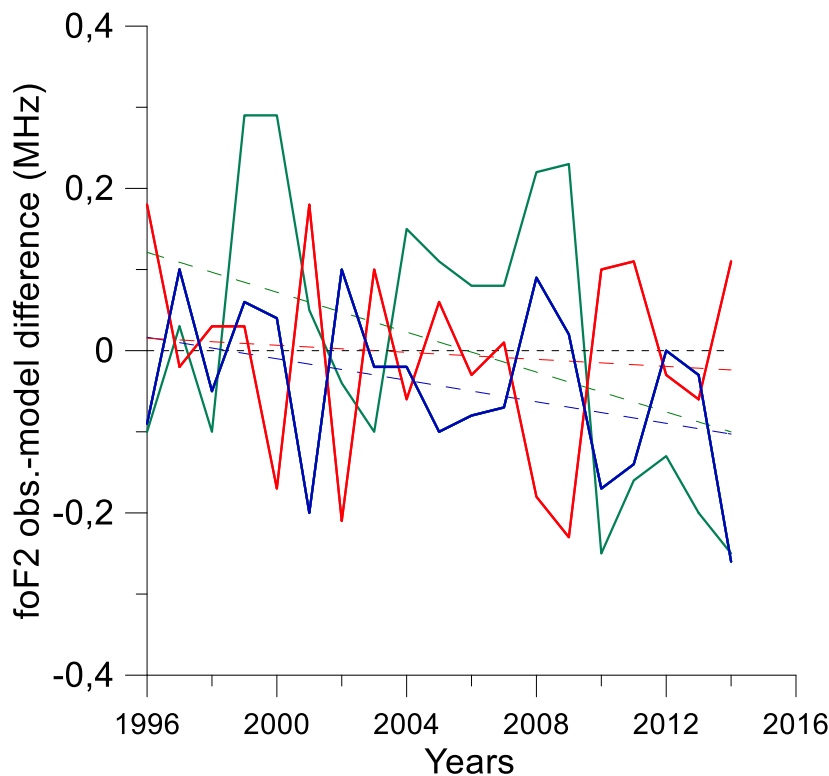


Fig. 13. Differences between observed and model (Eq. (1)) yearly values of foF2 for Pruhonice, 1996–2014. Green curve - solar activity proxy F10.7; blue curve – solar proxy F30; red curve – solar proxy Mg II; longer-dash colored lines – respective linear trends; short-dash black horizontal line – zero difference level. A negative difference means smaller observed than model value.

Laštovička, J. (2021a). What is the optimum solar proxy for long-term ionospheric investigations? *Adv. Space Res.*, 67, 2-8, <https://doi.org/10.1016/j.asr.2020.07.025>.

Laštovička, J. (2021b). The best solar activity proxy for long-term ionospheric investigations *Adv. Space Res.*, 68, 2354-2360, <https://doi.org/10.1016/j.asr.2021.06.032>.

Astronomical Institute of the Czech Academy of Sciences (AI CAS):

Hard X-ray imaging spectroscopy. The Spectrometer/Telescope for Imaging X-rays (STIX) is the hard X-ray instrument onboard the Solar Orbiter. STIX uses hard X-ray imaging spectroscopy in the range between 4-150 keV to diagnose the hottest flare plasma and related non-thermal electrons. The first-result paper focused on the temporal and spectral evolution of micro-flares occurring in the Active Region (AR) AR12765 in June 2020, and compares the STIX measurements with Earth-orbiting observatories such as the X-ray Sensor of the Geostationary Operational Environmental Satellite (GOES/XRS), the Atmospheric Imaging Assembly of the Solar Dynamics Observatory (SDO/AIA), and the X-ray Telescope of the Hinode mission. For the observed micro-flares of the GOES A and B class, the STIX peak time at lowest energies is located in the impulsive phase of the flares, well before the GOES peak time. Such a behavior can either be explained by the higher sensitivity of STIX to higher temperatures compared to GOES, or due to the existence of a non-thermal component reaching down to low energies. For the largest flare in the sample, the low-energy peak time is clearly due to thermal emission, and the non-thermal component seen at higher energies occurs even earlier. This suggests that the classic thermal explanation might also be favored for the majority of smaller flares. In combination with EUV and soft X-ray observations, STIX corroborates earlier findings that an isothermal assumption is of limited validity.

Commissioning observations confirm that STIX is working as designed. As a rule of thumb, STIX detects flares as small as the GOES A class. For flares above the GOES B class, detailed spectral and imaging analyses can be performed.

After the commissioning phase the Metis coronagraph onboard the Solar Orbiter provided first-light observations in mid-2020. They have proven an excellent quality of the imaging system with two main mirrors made in the Czech Republic. During the cruise phase several observations in both Metis channels have been successfully obtained. We performed cosmic-ray flux predictions and observations, first light observations of the solar wind in the outer corona, the first coronal mass ejection observed in both visible-light (VL) and UV H I Ly- α channels, and observations of a coronal mass ejection followed by a prominence eruption and a plasma blob. Several papers using this data have been already published by the whole Metis consortium. Recently two extremely large prominence eruptions have been detected by Solar Orbiter, together with other space instruments (STEREO, SDO/AIA) and the rich data is now being processed. In 2020 the team of AI CAS suggested that the Metis VL channel can also provide an important plasma and magnetic-field diagnostics using the helium 587.6 nm line which can contribute to total signal detected by the VL channel and also to polarized brightness.

Faculty of Mathematics and Physics of the Charles University (FMP CU):

Propagation of electromagnetic signals radiated by Alpha navigation transmitters. We investigated propagation at frequencies of 11.9, 12.6 and 14.9 kHz. The radiated signals propagate through the magnetosphere to the conjugate hemisphere, where they are detectable by the low-altitude DEMETER spacecraft. Due to a Doppler shift, the observed frequencies are at times rather different than the radiated frequencies, indicating a propagation at large wave normal angles. Simultaneous observations of signals with different Doppler shifts allowed us to distinguish three distinct ways of propagation: i) ducted propagation, ii) non-ducted propagation, and iii) partially ducted propagation. A raytracing analysis was used to reveal typical wave trajectories, and the calculated Doppler shifts agreed with the observed ones. Our results demonstrate the complicated ways of signal propagation throughout the magnetosphere and the possibility of using Doppler shifts to obtain wave normal angles.

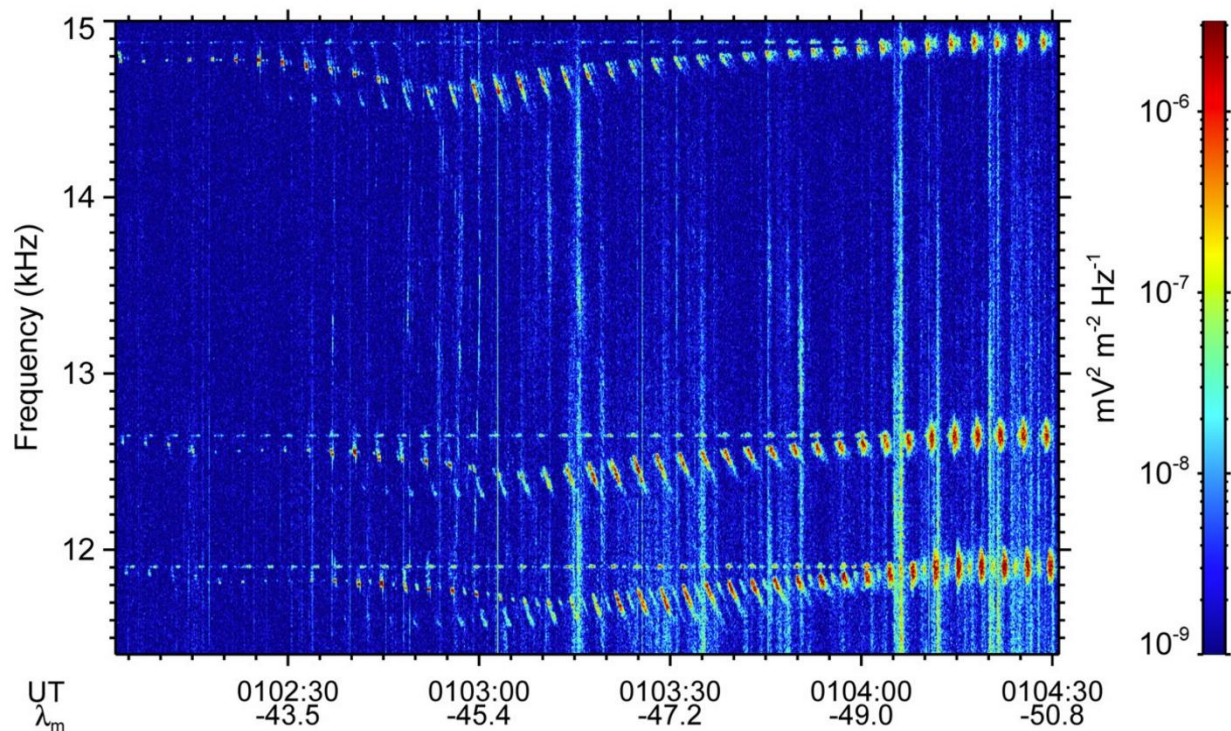


Fig. 14. Frequency-time spectrogram of power spectral density of electric field fluctuations corresponding to one of the analyzed events, when the spacecraft was located in the hemisphere conjugate to the transmitter. The discrete transmission pattern of the Alpha transmitter can be seen at 11.9, 12.6, and 14.9 kHz. Additionally, Doppler-shifted transmitter signals with gradually decreasing and later increasing frequencies are observed in addition to the expected constant-frequency signals.

F. Němec, O. Santolík, M. Parrot: Doppler shifted Alpha transmitter signals in the conjugate hemisphere: DEMETER spacecraft observations and raytracing modeling. *J. Geophys. Res. Space Physics*, 126, e2020JA029017, doi: 10.1029/2020JA029017, 2021.

Dust impact detection. Detection by electric field instruments is a well-established technique, but not all aspects of signal generation by dust impacts are completely understood. We presented a study of events related to dust impacts on the spacecraft body detected by electric field probes operating simultaneously in the monopole (probe-to-spacecraft potential measurement) and dipole (probe-to-probe potential measurement) configurations by the Earth-orbiting Magnetospheric Multiscale mission spacecraft. This unique measurement allows us to investigate connections between monopole and dipole data. Our analysis shows that the signal detected by the electric field instrument in a dipole configuration is generated by an ion cloud expanding along the electric probes. In this case, expanding ions affect not only the potential of the spacecraft body but also one or more electric probes at the end of antenna booms. Electric probes located far from the spacecraft body can be influenced by an ion cloud only when the spacecraft is located in tenuous ambient plasma inside of the Earth's magnetosphere. Derived velocities of the expanding ions on the order of tens of kilometers per second are in the range of values measured experimentally in the laboratory.

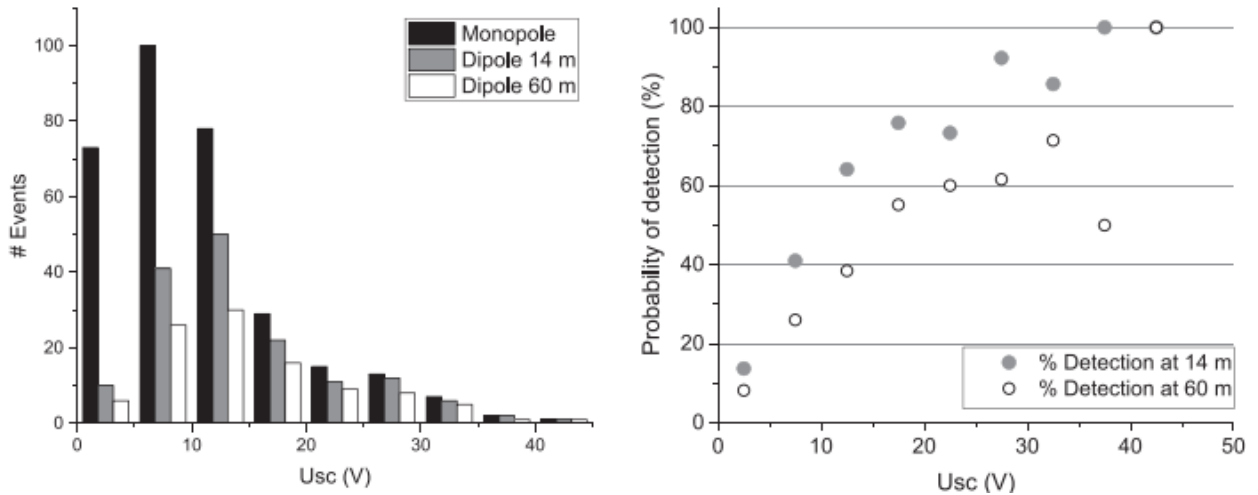


Fig. 15. The number of events detected in monopole and dipole configurations for probes located 14 and 60 m from the spacecraft body as a function of the spacecraft potential, U_{sc} (left panel). The probability of signal detection by dipole probes as a function of the spacecraft potential (right panel).

J. Vaverka, J. Pavlů, L. Nouzák, J. Šafránková, Z. Němeček, T. Antonse, I. Mann, and P-A. Lindqvist: Ion Cloud Expansion after Hyper-velocity Dust Impacts Detected by the Magnetospheric Multiscale Mission Electric Probes in the Dipole Configuration, *Astrophysical Journal*, 921:127 (8pp), doi: 10.3847/1538-4357/ac1944, 2021.

Fluctuation anisotropy in minimum variance frames of the magnetic field and solar wind velocity. We present a large statistical study of the fluctuation anisotropy in minimum variance (MV) frames of the magnetic field and solar wind velocity. We use 2, 10, 20, and 40 minute intervals of simultaneous magnetic field (the Wind spacecraft) and velocity (the Spektr-R spacecraft) observations. Our study confirms that magnetic turbulence is a composite of fluctuations varying along the mean magnetic field and those changing in the direction perpendicular to the mean field. Regardless of the length scale within the studied range of spacecraft-frame frequencies, $\approx 90\%$ of the observed magnetic field fluctuations exhibit an MV direction aligned with the mean magnetic field, $\approx 10\%$ of events have the MV direction perpendicular to the background field, and a negligible portion of fluctuations has no preferential direction. On the other hand, the MV direction of velocity fluctuations tends to be distributed more uniformly. An analysis of magnetic compressibility and density fluctuations suggests that the fluctuations resemble properties of Alfvénic fluctuations if the MV direction is aligned with background magnetic field whereas slow-mode-like fluctuations have the MV direction perpendicular to the background field. The proportion between Alfvénic and slow-mode-like fluctuations depends on plasma β and length scale: the dependence on the solar wind speed is weak. We present 3D numerical MHD simulations and show that the numerical results are compatible with our experimental results.

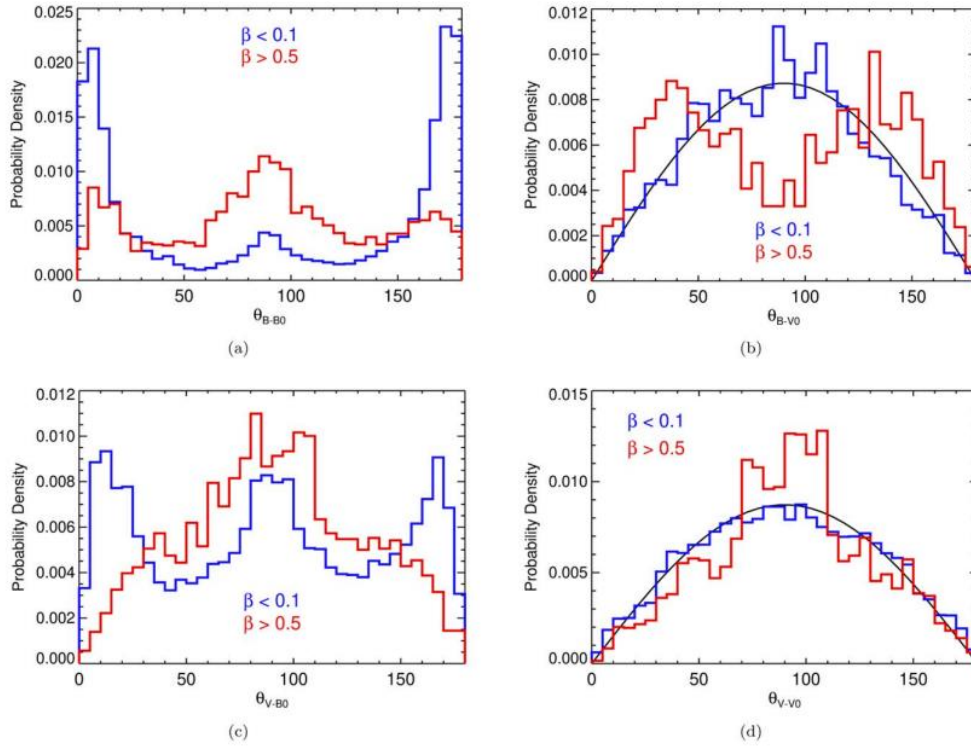


Fig. 16. Top panels—distributions of angles between the MVB direction and background magnetic field, Θ_{B-B0} (left) and mean solar wind bulk velocity, Θ_{B-V0} (right). Bottom panels—distributions of angles between the MVV direction and background magnetic field, Θ_{V-B0} (left) and mean solar wind bulk velocity, Θ_{V-V0} (right). In both right panels, black color curves correspond to random distributions.

J. Šafránková, Z. Němeček, F. Němec, V. Montagud-Camps, D. Verscharen, A. Verdini, T. Durovcová: Anisotropy of Magnetic Field and Velocity Fluctuations in the Solar Wind, *Astrophysical Journal*, 913:80 (12pp), doi: 10.3847/1538-4357/abf6c9 (2021).